HHS Public Access

Author manuscript

Opt Lett. Author manuscript; available in PMC 2016 April 15.

Published in final edited form as:

Opt Lett. 2015 April 15; 40(8): 1779–1782.

4D Optical Coherence Tomography based Microangiography achieved by 1.6 MHz FDML Swept source

Zhongwei Zhi[1], **Wan Qin**[1], **Jingang Wang**[1], **Wei Wei**[1], and **Ruikang K. Wang**[1,2,*]

[1]Department of Bioengineering, University of Washington, Seattle, WA 98195, USA

[2]Department of Ophthalmology, University of Washington, Seattle, WA 98195, USA

Abstract

We demonstrate the use of an ultra-high speed swept-source optical coherence tomography (OCT) to achieve optical microangiography (OMAG) of microcirculatory tissue beds *in vivo*. The system is based on a 1310 nm Fourier domain mode locking (FDML) laser with 1.6MHz A-line rate, providing a frame rate of 3.415 KHz, an axial resolution of ~10 μm and signal to noise ratio of 102 dB. Motion from blood flow causes change in OCT signals between consecutive B-frames acquired at the same location. Intensity based inter-frame subtraction algorithm is applied to extract blood flow from tissue background without any motion correction. We demonstrate the capability of this 1.6 MHz OCT system for 4D optical microangiography of *in vivo* tissue at a volume rate of 4.7 volumes/s (volume size: 512×200×720 voxels).

Optical coherence tomography (OCT) [1] is a well-established noninvasive imaging modality that is capable of three-dimensional (3D) imaging of biological tissues at micrometer scale resolution. The development of Fourier domain OCT provides markedly increased imaging speeds and sensitivity [2], enabling *in vivo* imaging of blood flow. Optical microangiography (OMAG) [3] is one of the earliest proposed OCT angiography methods capable of generating 3D images of dynamic blood perfusion distribution within microcirculatory tissue beds. An unprecedented sensitivity to the blood flow down to 4μm/s was reported with the development of an ultrahigh sensitive OMAG [4, 5]. One of the main limitations of OCT based microangiography for *in vivo* tissue microcirculation imaging is the motion artifact. There are many approaches proposed to minimize the motion. The most effective way is to increase the imaging speed of OCT. Efforts in developing new sweeping laser sources pushed the OCT speed into mutli-MHz A-line rate era [6] and live 3D OCT microstructure imaging at video rate has been demonstrated [7]. However, all these previous efforts are focused on using the ultra-high speed OCT for *in vivo* tissue microstructure imaging.

Here, we demonstrate that the commercially available 1.6 MHz Fourier domain mode locked (FDML) swept laser source (Optores GmbH, Germany) [6, 7] enables OCT based microangiography to achieve 3D and 4D imaging of tissue microvasculature without any motion correction. To the best of our knowledge, this is the first study that reports the

*Corresponding author: wangrk@uw.edu.

utilization of MHz OCT system to perform 3D and 4D imaging of microcirculations within tissue beds *in vivo*.

The schematic of the ultra-high speed swept source OCT (SS-OCT) system is shown in Fig. 1. The system is based on a 1310nm FDML laser with 1.6MHz A-line rate. This light source can provide a tunable output power and wavelength bandwidth. In this setup, we used an output power of 60 mW with a spectral scanning range of 110 nm. The light from the laser was split by a 90/10 coupler with 10% to the reference arm. The 90% arm was further divided into sample and recalibration arms by a 99/1 coupler. The 1% light was used to interfere with the reference arm for recalibration. The interference signal after the 50/50 coupler was collected by Thorlabs PDB480C-AC balanced photoreceiver (1.6 GHz bandwidth) and digitized by a 12-bit digitizer (ATS9360, Alazartech) at 1.8 GS/s. In the sample arm, in order to achieve fast scanning speed and fully utilize the speed of light source, a 3.415 kHz resonant scanner (SC-30, EOPC) was employed for fast axis scan, meaning the frame rate of the data acquisition was fixed at 3415 frames/s, resulting in a theoretical depth scans of 236 per frame. In the slow scan axis, we used a Galvo scanner (6215H, Cambridge Technology). The beam was focused with a 5× scanning lens (SLM03, Thorlabs, Inc.), providing a theoretical beam size of ~14 μm at the focus spot. The axial resolution in air was about 10 μm and the system sensitivity was measured to be 102 dB at the focus depth position with light power in the sample arm at approximately 15 mW.

The new FDML source makes resampling as easy as in spectral-domain OCT and no k-clock was required [7]. The recalibration arm was used to determine the parameters for resampling. Fig. 2 (a–b) shows the typical interference fringe signal recorded for recalibration with Thorlabs PDB480C-AC balanced photoreceiver and digitized by Alazartech ATS9360 ADC at 1.8GS/s. Fig. 2 (c) shows sensitivity rolling-off curve of the system runs at 1.6 MHz line rate. The total imaging depth is ~4mm and there is ~3 dB sensitivity loss at 2 mm depth.

In order to achieve microangiography, an OMAG scanning protocol [8, 9] which requires multiple B-scans taken at the same location was utilized. Since the depth scans at the turning points of scanner are not useful for imaging, the effective duty-cycle of the B-frame was ~85%, resulting in an actual usable 200 depth scans for each B-frame. In the slow-scan axis, 2000 B-frames were captured at 200 locations (10 frames per location). With the frame rate at 3.415 kHz, it took 0.6 second to finish one 3D scan. The raw OCT data acquired was processed to obtain OCT structural image through the following steps: resampling with a 3rd order Hermite kernel, apodizing to Hann shape, fast Fourier transform (FFT) with 1024 samples, dynamic range compression (logarithm of magnitude) and finally cut level clipping [7].

In order to obtain blood flow images, we applied the algorithm: intensity-based inter-frame subtraction onto the OCT structural images [10] i.e.

$$I_{flow}(j,k)=\frac{1}{N-1}\sum_{i=1}^{N-1}\left|\left(I_{str}(i+1,j,k)-I_{str}(i,j,k)\right)\right| \quad (1)$$

where *N* specifies the number of frames acquired at the same location and *i*, *j*, and *k* are indices for the frame, transverse, and axial pixels, respectively.

To demonstrate the capability of the MHz SS-OCT system for high definition 3D optical microangiography, we conducted experiments to image the tissue microvasculature of mouse brain and human skin *in vivo*. The scanning protocol described above was first applied to capture a 3D data cube that covered ~2× 2 mm^2 on mouse brain through cranial window. Fig. 3 (a) shows a representative B-scan image of microstructure in mouse brain and Fig. 3 (b) gives the corresponding blood flow image. The high system SNR and weak sensitivity roll-off enables deep imaging into the brain, for example the functional blood vessels (yellow arrows) supplying a region close to hippocampus within white matter can be visualized clearly. Fig. 3 (c) gives the OMAG image of cerebral microcirculation where abundant large blood vessels and capillaries could be visualized. Fig. 3 (d) illustrates a 3D view of the cortical microvasculature and blood vessels within the white matter were pointed by yellow arrows.

Inter-frame calculation based OCT angiography techniques are strongly affected by bulk tissue motion due to the increased time interval necessary for imaging slow blood flows. Motion correction is often required for OCT angiography of human subjects, such as on skin and retina [11, 12]. Here, we demonstrate that the ultrahigh speed OCT system enables microangiography of skin tissue of non-stabilized finger without motion correction. This is enabled by fast 3D data acquisition, which takes only 0.6s in this study. The system was applied to image the microvasculature change after accidental wound in the fingertip skin of a volunteer subject. The finger was placed under the beam without any stabilization measures applied. Fig. 4 shows the result of microvascular pattern at 2 days after a wound cut to the fingertip (Fig. 4c). From the OMAG images (Fig. 4 (e–f)), the capillary vessels were dropped out at the damaged region while more capillaries are seen at the adjacent region, presumably due to the vessel remodeling during wound healing phase. In order to better show this, we zoomed into three different regions: wound center (yellow), adjacent region (white) and normal region (blue) and counted the number of capillary loops per mm^2 within each region (fig. 4 (g)). The capillary density and capillary loop size were increased in the adjacent region as compared to normal region.

The temporal resolution is a key parameter for the investigation of blood flow dynamics in some specific applications. 4D imaging of the microcirculation would provide important information regarding the fast processes that have vascular involvement. In order to demonstrate the capability of the ultra-high speed SS-OCT system for 4D blood flow imaging, we imaged the fast response after the release of blockage of root artery and vein in mouse ear. The root artery supply all the blood for the ear and the root vein drains them back to heart. The scan along the slow axis is performed in uni-directional manner with a modified sawtooth waveform at 4.7 Hz. For each 3D volume, 720 frames were captured at 180 cross-sectional locations (4 B-scans per location). 25 volumes (volume size: 512×200×720 voxels) were captured immediately after the blockage was released. The algorithm described above (Eq.(1)) was applied to obtain blood flow images for each 3D volume. To better show the result, the mean intensity projection view of 3D flow images are calculated and streamed as a movie (Media 1).

Blood reperfusion dynamics was observed with high temporal resolution of 0.21s that the system offers. Frames were extracted from the movie to show several critical steps (Fig. 5). At frame #1 (0.21s), we observe that venules (yellow arrows) first start to flow before the arterioles (red arrow) after the release of the blockage. The arterial flow begins at 0.42s where only portion of the arteriole is observed with flow signal. At 0.63s, the whole arteriole is fully functional while the vein is seen with markedly reduced flow. The blood flow in both arterioles and venules returned to the normal state after ~2 seconds. Based on our observation, we interpret the blood flow response as: upon the release of the root vessel blockage, the deoxygenated blood within ischemic region is first drained back to heart via venule system; arterioles then bring oxygenated blood to the ischemic tissue region and finally the venules coordinate with the arteriole flow in order to balance the blood supply and drainage. Interestingly, we found a venule shunts (closed yellow arrow) that works only temporary during the reperfusion.

In summary, we have constructed an ultra-high speed SS-OCT system featured with 1.6 MHz sweeping rate FDML source and demonstrate its capability for 3D and 4D optical microangiography of *in vivo* tissue. The system provides an axial resolution of ~10 μm and SNR of 102 dB. Intensity-based inter-frame subtraction was used to extract blood flow from background tissue. No motion correction is required owing to the ultra-high speed acquisition provided by the light source. The performance of the system for microvasculature imaging was demonstrated by showing high definition 3D blood vessel networks obtained from a mouse brain *in vivo* and human finger skin after wound. We also demonstrate the system capability for 4D imaging of blood flow dynamics at volume rate of 4.7 volumes/s (volume size: 512×200×720 voxels) on mouse ear. Promising future applications could be expected from this ultrahigh speed SS-OCT system for non-invasive and non-contact investigation of fast structural and microvascular changes during complicated tissue conditions, either for humans or small animals. Graphics processing unit (GPU) accelerated OCT processing has been reported that enables video rate volumetric rendering [13]. In the future, we plan to apply GPU processing to enable real-time 4D blood flow imaging and display with this system.

Acknowledgments

We would like to acknowledge the technical assistance provided by Dr Wolfgang Wieser from Optores GmbH, Germany, in the setting up of the system used in this study. This work was supported in part by research grants from the National Heart, Lung, and Blood Institute (R01 HL093140) and National Institute of Biomedical Imaging and Bioengineering (R01 EB009682). The content is solely the responsibility of the authors and does not necessarily represent the official views of grant giving bodies.

Reference

1. Huang D, Swanson EA, Lin CP, Schuman JS, Stinson WG, Chang W, Hee MR, Flotte T, Gregory K, Puliafito CA. Optical coherence tomography. Science. 1991; 254:1178–1181. [PubMed: 1957169]
2. Leitgeb R, Hitzenberger CK, Fercher AF. Performance of fourier domain vs. time domain optical coherence tomography. Opt Express. 2003; 11:889–894. [PubMed: 19461802]
3. Wang RK, Jacques SL, Ma Z, Hurst S, Hanson SR, Gruber A. Three dimensional optical angiography. Optics Express. 2007; 15:4083–4097. [PubMed: 19532651]

4. An L, Qin J, Wang RK. Ultrahigh sensitive optical microangiography for in vivo imaging of microcirculations within human skin tissue beds. Opt. Express. 2010; 18:8220–8228. [PubMed: 20588668]
5. Zhi ZW, Chao JR, Wietecha T, Hudkins KL, Alpers CE, Wang RKK. Noninvasive Imaging of Retinal Morphology and Microvasculature in Obese Mice Using Optical Coherence Tomography and Optical Microangiography. Invest Ophth Vis Sci. 2014; 55:1024–1030.
6. Wieser W, Biedermann BR, Klein T, Eigenwillig CM, Huber R. Multi-Megahertz OCT: High quality 3D imaging at 20 million A-scans and 4.5 GVoxels per second. Opt Express. 2010; 18:14685–14704. [PubMed: 20639955]
7. Wieser W, Draxinger W, Klein T, Karpf S, Pfeiffer T, Huber R. High definition live 3D-OCT in vivo: design and evaluation of a 4D OCT engine with 1 GVoxel/s. Biomed Opt Express. 2014; 5:2963–2977. [PubMed: 25401010]
8. Zhi ZW, Jung YR, Jia YL, An L, Wang RKK. Highly sensitive imaging of renal microcirculation in vivo using ultrahigh sensitive optical microangiography. Biomed Opt Express. 2011; 2:1059–1068. [PubMed: 21559119]
9. Wang RK, An L, Francis P, Wilson DJ. Depth-resolved imaging of capillary networks in retina and choroid using ultrahigh sensitive optical microangiography. Opt Lett. 2010; 35:1467–1469. [PubMed: 20436605]
10. Zhi ZW, Cepurna W, Johnson E, Shen T, Morrison J, Wang RKK. Volumetric and quantitative imaging of retinal blood flow in rats with optical microangiography. Biomed Opt Express. 2011; 2:579–591. [PubMed: 21412463]
11. An L, Shen TT, Wang RKK. Using ultrahigh sensitive optical microangiography to achieve comprehensive depth resolved microvasculature mapping for human retina. J Biomed Opt. 2011; 16
12. Watanabe Y, Takahashi Y, Numazawa H. Graphics processing unit accelerated intensity-based optical coherence tomography angiography using differential frames with real-time motion correction. J Biomed Opt. 2014; 19
13. Jian YF, Wong K, Sarunic MV. Graphics processing unit accelerated optical coherence tomography processing at megahertz axial scan rate and high resolution video rate volumetric rendering. J Biomed Opt. 2013; 18

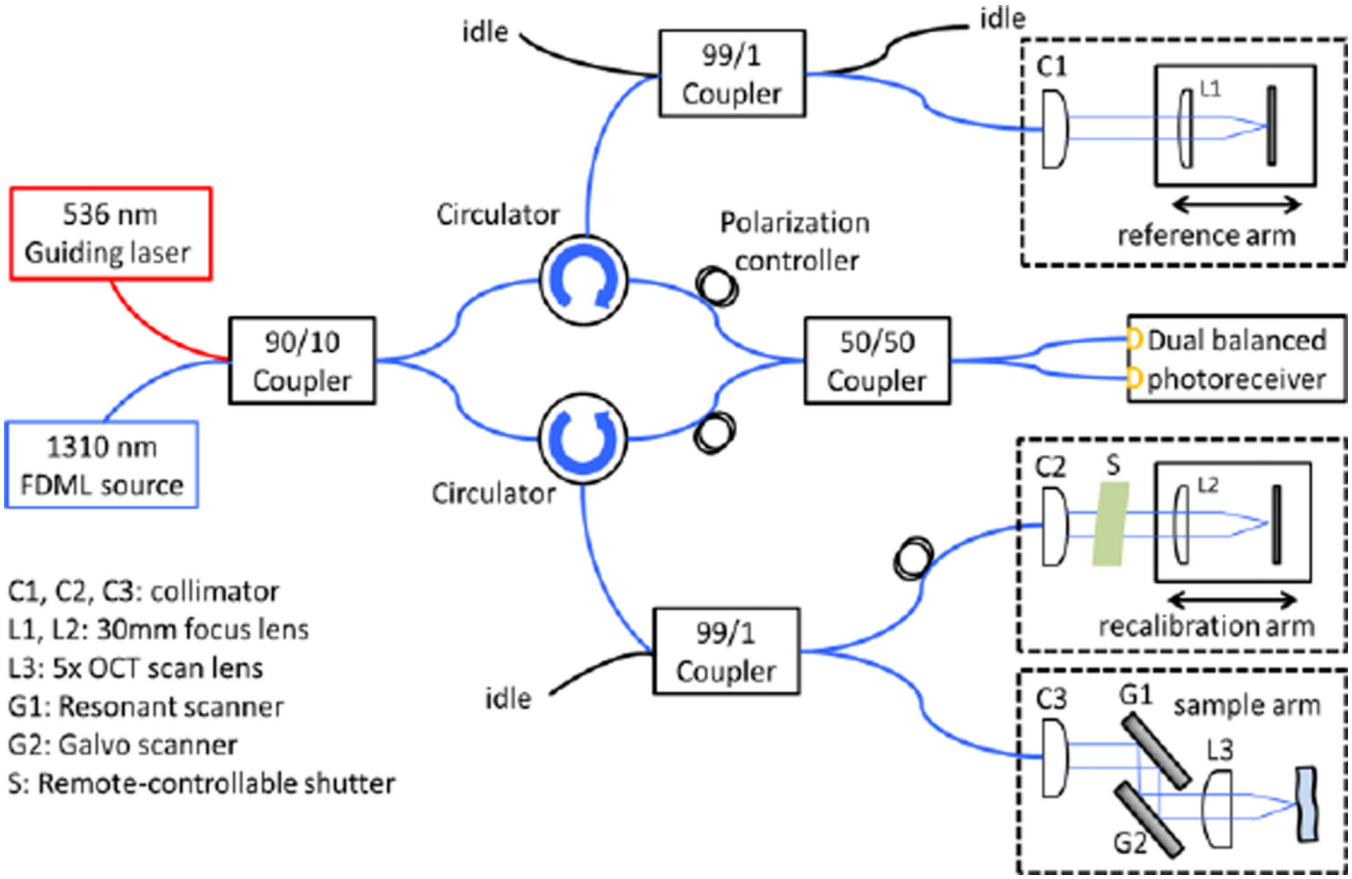

Fig. 1.

Schematics of the home-built OCT system featured with FDML light source at 1.6 MHz sweeping rate.

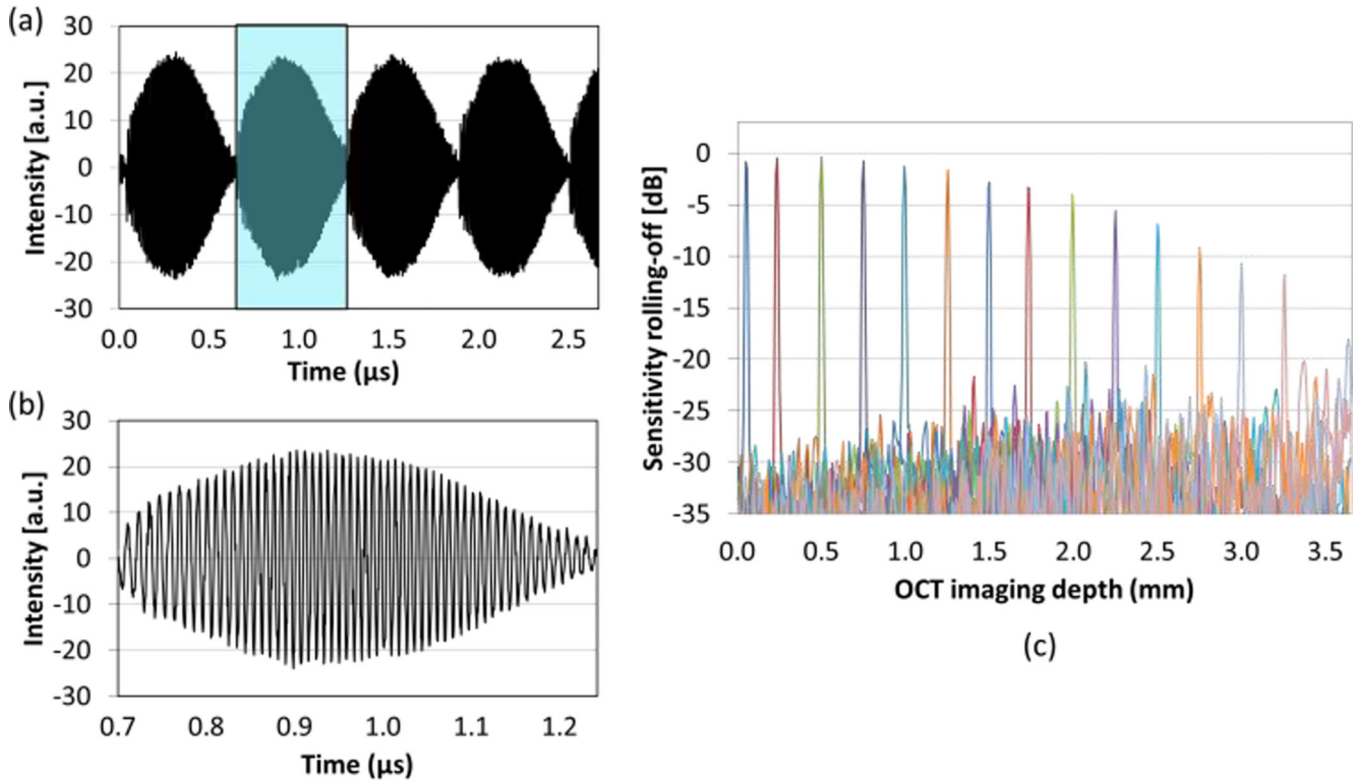

Fig. 2.

(a) The interference fringe signal, 4× buffered unidirectional sweeps were shown. (b) Zoom-in section of one sweep. (c) The system sensitivity roll-off curve at 1.6 MHz sweeping rate, with 3dB falling off measured at 2 mm depth.

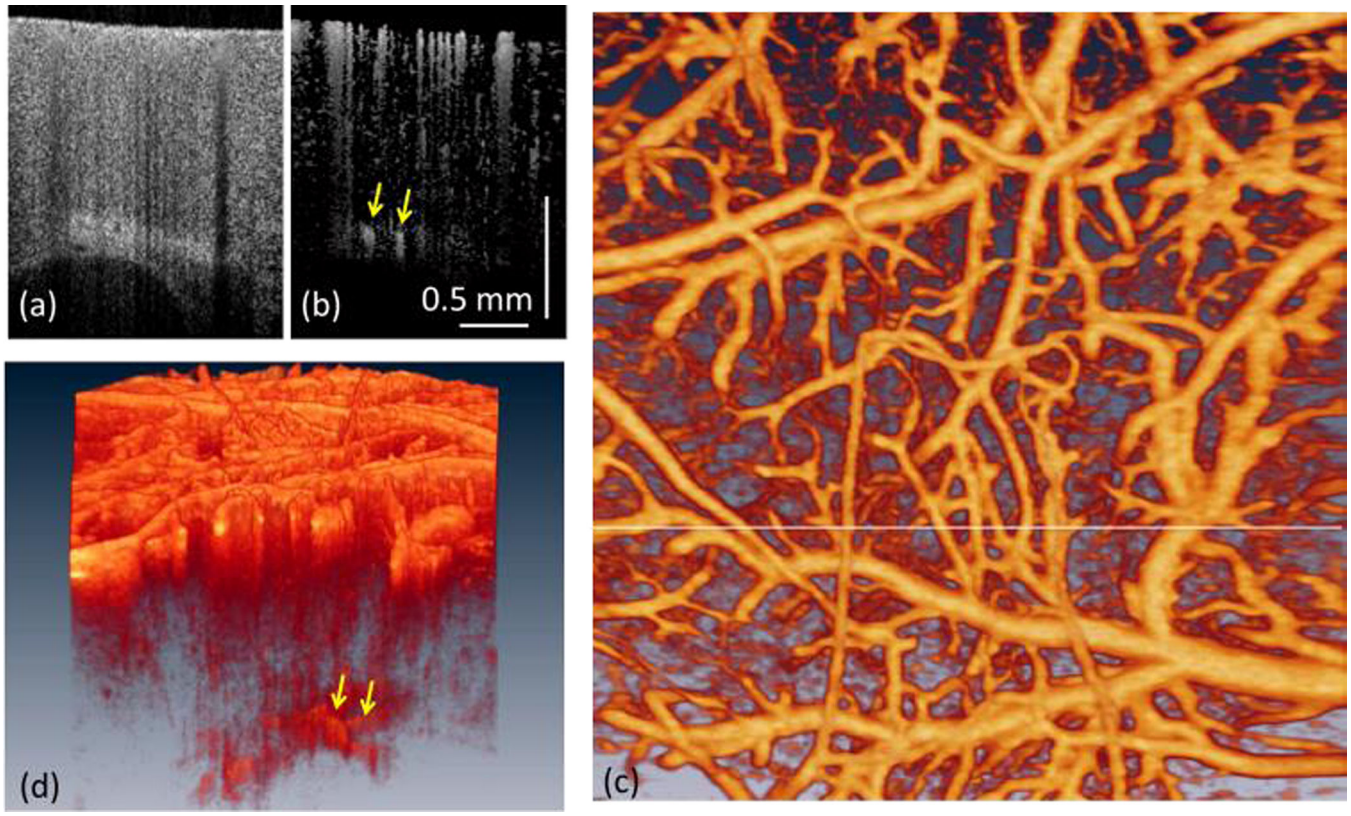

Fig. 3.

(a) Cross-sectional structural image of mouse brain and (b) corresponding blood flow image. (c) En face view of the 3D microangiogram, white line indicates the position of cross-sectional images, image size: 2 × 2 mm^2. (d) 3D volume rendering of the cerebral microvasculature. Yellow arrows point to the vessels located within white matter.

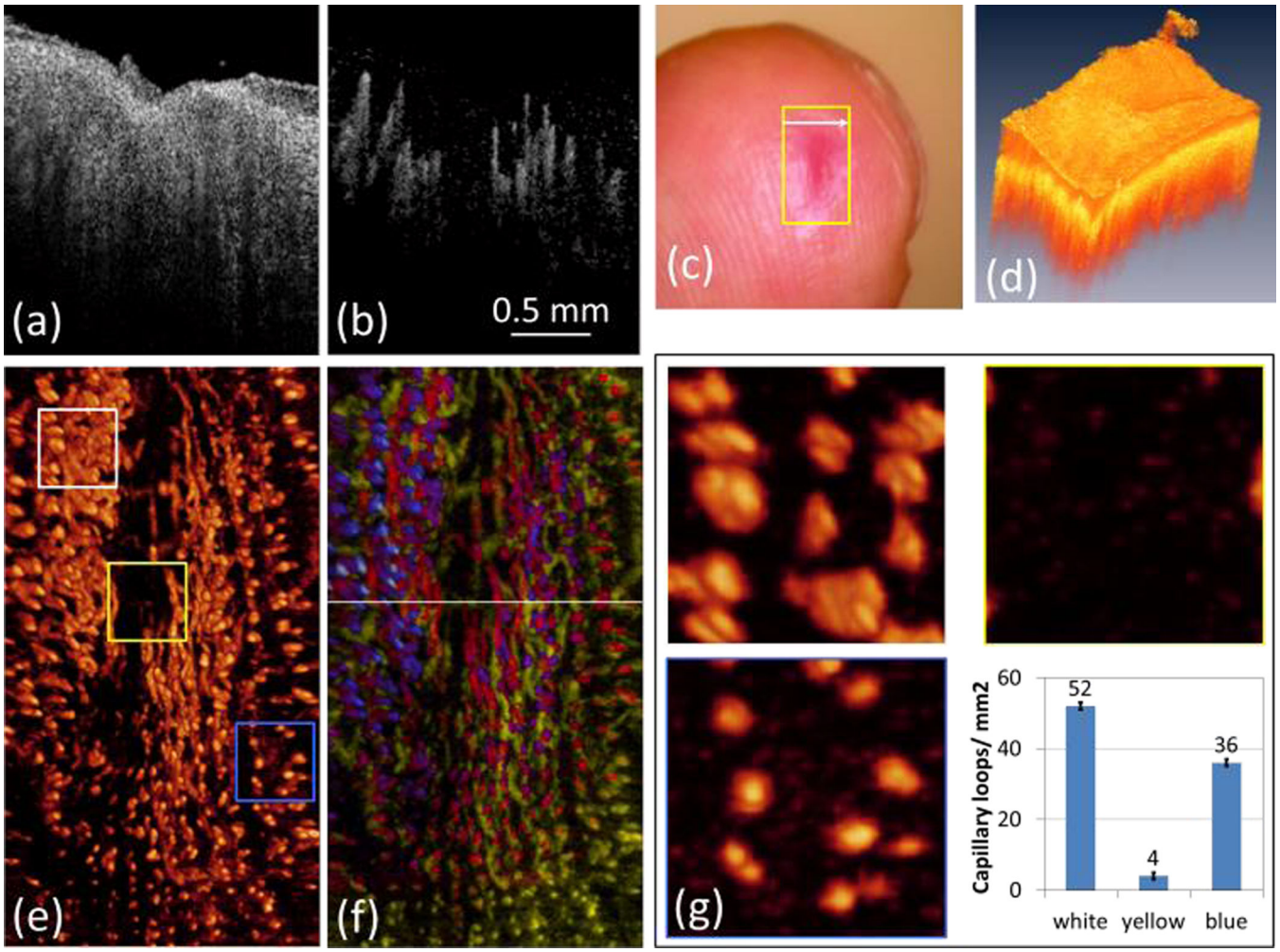

Fig. 4.

Microvasculature of human fingertip after accident tissue damage. (a) Cross-sectional structural image of wound region and (b) corresponding blood flow image. (c) Photo shows the finger with the yellow square indicate where the 3D OCT data was taken. (d) 3D rendering of the structure. (e) *En face* view of the 3D microvasculature. (f) Depth-encoded map of the microvasculature, pink: top red: medium yellow: bottom. Image size of (d, e, f): 2×3.5 mm^2 (g) Zoom-in view of the capillary loops in the square region outlined in (e), and bars indicate the number of capillary loops per mm^2. The size of each square region = 0.5 × 0.5 mm^2

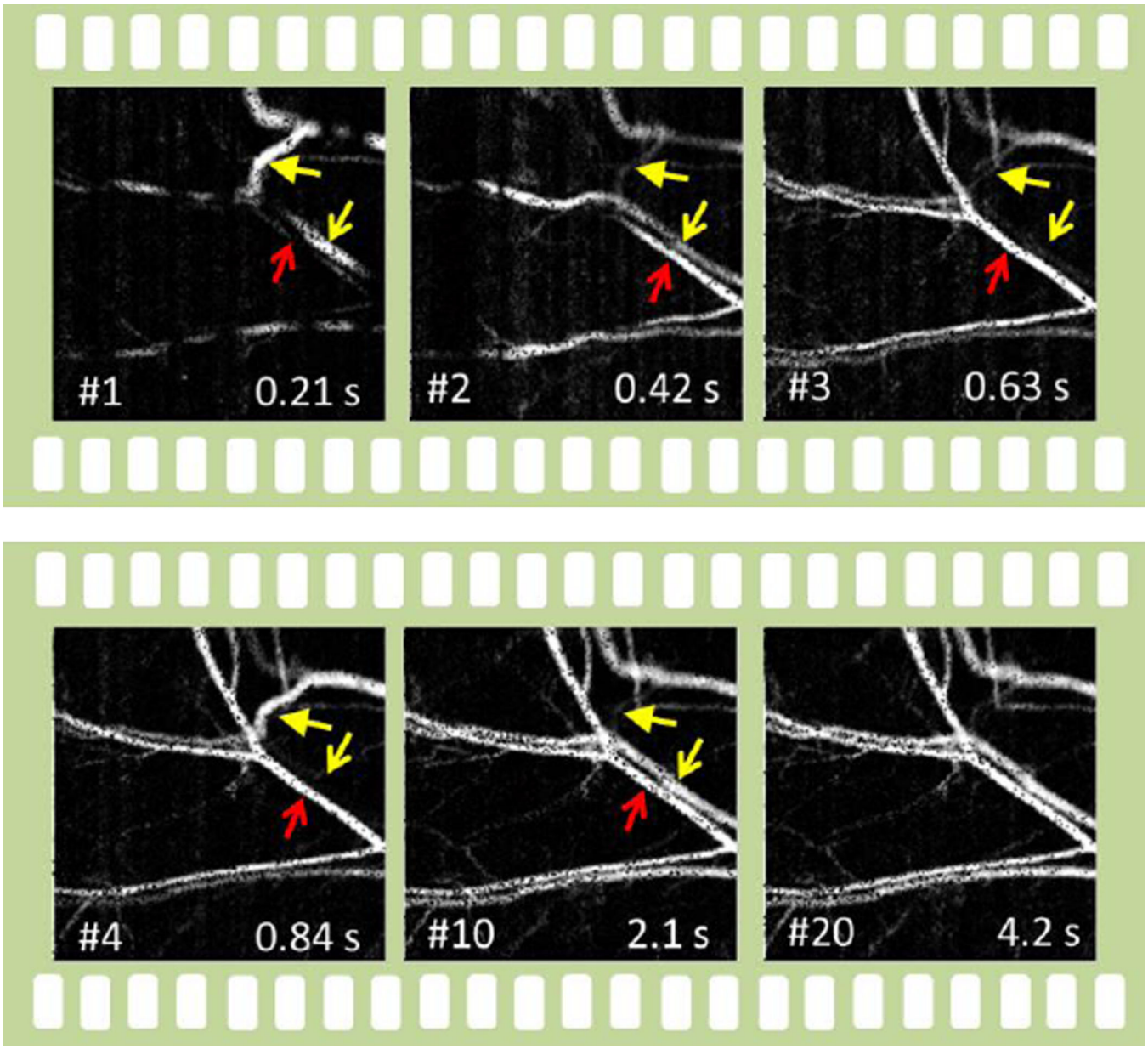

Fig. 5.

Frames taken from a 4D movie (Media 1): the blood flow response after the release of blockage of large artery and vein in the mouse ear. The blood flows back to heart first before the blood flow to the peripheral ear through artery and then the vein starts to flow. Yellow arrow: vein, red arrow: artery.